Title

DEVELOPMENT OF A 100-ma PROTON SOURCE AND LENS SYSTEM FOR THE BEVATRON MARK-II INJECTOR

Authors

Allison, Robert W.
Cork, Bruce
Richter, Robert M.
et al.

Publication Date

1961-06-12

Arc

UCRL 9743

UNIVERSITY OF CALIFORNIA

Ernest O. Lawrence

Radiation Laboratory

DEVELOPMENT OF A 100-ma PROTON SOURCE AND LENS SYSTEM FOR THE BEVATRON MARK-II INJECTOR

UCRL-9743
UC-28 Particle Accelerators
and High-Voltage Machines
TID-4500 (16th Ed.)

UNIVERSITY OF CALIFORNIA

Lawrence Radiation Laboratory
Berkeley, California

Contract No. W-7405-eng-48

DEVELOPMENT OF A 100-ma PROTON SOURCE AND LENS SYSTEM FOR THE BEVATRON MARK-II INJECTOR

Robert W. Allison, Jr., Bruce Cork, Robert M. Richter,
Joseph F. Smith, Glenn E. White, and Emery Zajec

June 12, 1961

Printed in USA. Price $1.00. Available from the
Office of Technical Services
U. S. Department of Commerce
Washington 25, D.C.

DEVELOPMENT OF A 100-ma PROTON SOURCE AND LENS SYSTEM FOR THE BEVATRON MARK-II INJECTOR

Contents

DEVELOPMENT OF A 100-ma PROTON SOURCE AND LENS SYSTEM FOR THE BEVATRON MARK-II INJECTOR

Robert W. Allison, Jr., Bruce Cork, Robert M. Richter,
Joseph F. Smith, Glenn E. White, and Emery Zajec
Lawrence Radiation Laboratory
University of California
Berkeley, California

June 12, 1961

I. INTRODUCTION

As part of the injector development program, a small Cockcroft-Walton accelerator was constructed and used as a test stand. On this stand we have developed a high-intensity ion source and a matching lens for the accelerating column. In addition some experiments have been made with a magnetic-beam confining system.

Results of this program, reported here, indicate that a preinjector can be built that will inject 85 ma of protons into the 18-Mev linear accelerator. Emittance measurements show that this beam will be accepted with a 1-cm-diam drift-tube bore.

II. TEST-STAND EQUIPMENT

Figure 1 is a block diagram of the test stand. Because of the slow column pumping speed, differential pumping is used. This is done by pumping at the ground end with two 200-liter sec^{-1} pumps (a Vac-ion, and a mercury diffusion pump) and at the high voltage end with a 125 liter sec^{-1} Vac-ion pump.

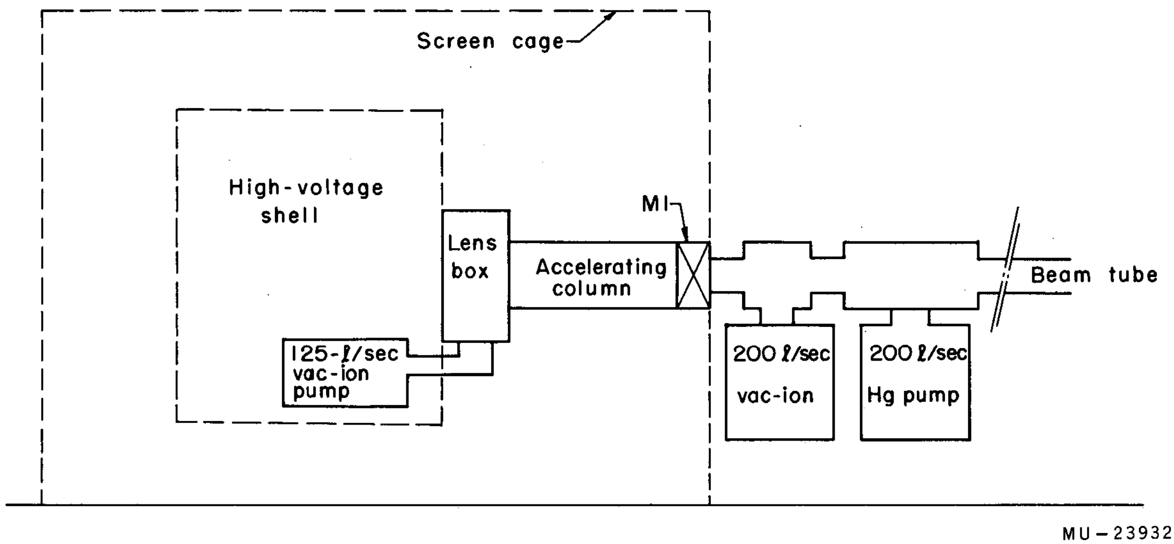

Fig. 1. Block diagram of test stand.

Additional equipment used includes a mass spectrograph, Faraday cups, and two beam-analyzing boxes. These boxes have cups and apertures that move in two dimensions and are used to measure beam emittance.

III. SOURCE ASSEMBLY AND CHARACTERISTICS

A duo-plasmatron ion source, designed for pulsed operation, has been constructed. This source is especially adaptable for use on large accelerators. All of the internal parts, including the extraction electrode, can be removed from the rear of the assembly. Removal, in this fashion, does not affect the preinjector electrode alignment.

Figure 2 is a cross section of the source. Five subassemblies are used. These are:

A. source body

B. aperture and extractor cone

C. middle electrode (snout)

D. filament assembly

E. extractor electrode.

A. Source Body

In Figure 2, the source body consists of a mild-steel face plate (1) which has a stainless steel tube (2) welded into it. A solenoid (3) slips over this tube and is held in place by a split ring (4). This clamp is recessed, providing alignment of the snout assembly.

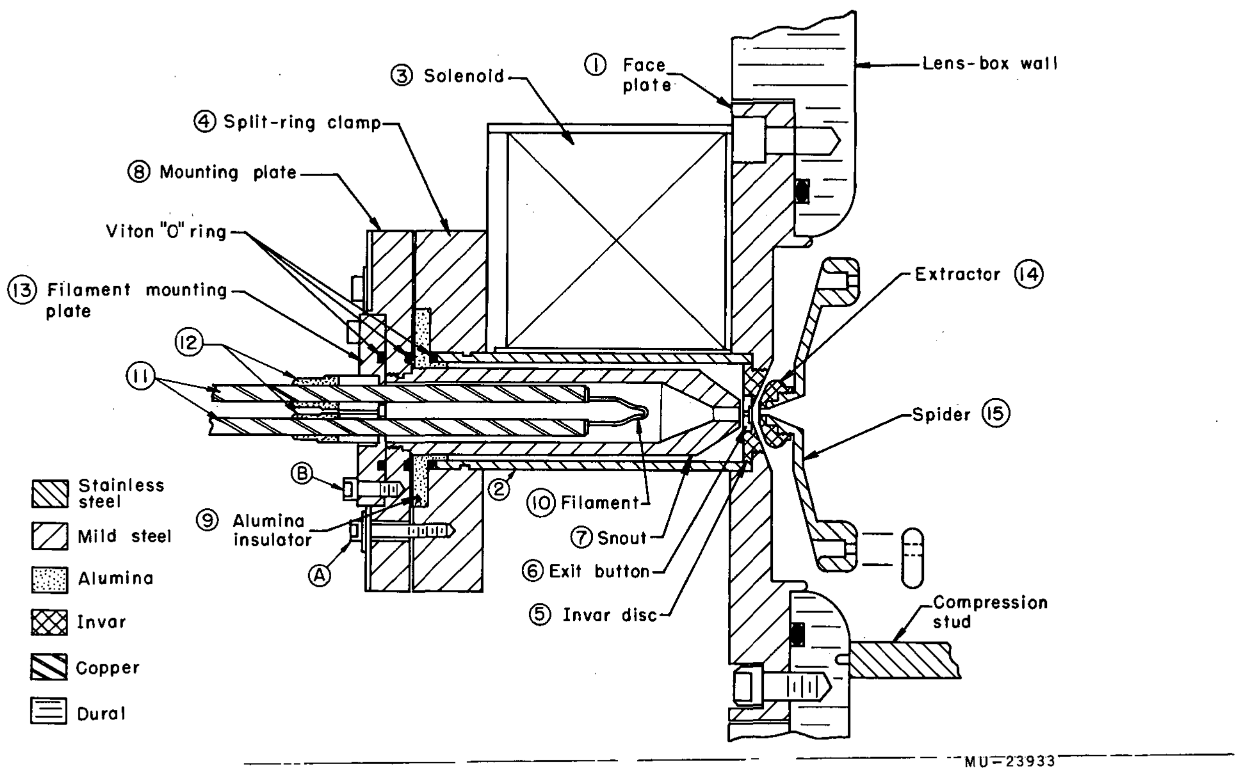

Fig. 2. Source detail.

The source body bolts onto the Cockcroft-Walton lens tank and is held in close alignment by a protruding lip. The face plate is threaded to receive the aperture assembly.

B. Aperture Assembly

This assembly is a cone-shaped invar disk (5) with a molybdenum cathode button (6) pressed into it. This button has a 0.020-in-diam and 0.024-in-deep aperture. The disk is aligned by a shoulder joint in the source body.

A spanner wrench, with a holding magnet, can be inserted in the disk to remove it. This wrench fits into the source body, and the assembly can be changed without removing the source body from the lens system.

C. Middle Electrode (Snout)

A mild-steel electrode (7), mounting plate (8), and an alumina insulator (9) form this assembly. The steel electrode is threaded into the mounting plate, and welded in place. Two 'O' rings and the insulator slip over the electrode, forming vacuum-tight joints between the mounting plate, insulator, and the rear of the source holder. Because of filament heat, Viton 'O' rings must be used. It should be noted that this is the weakest part of the design. We feel that having the source "inside" parts readily accessible justifies this complicated multiple 'O'-ring seal.

The snout assembly is aligned by the alumina insulator's fitting into the source split ring. This insulator is ground to ± 0.0005 in. on all diameters.

The magnetic path is through source plate (1), and the invar disk (5), across a 0.060-in. gap to the snout electrode (7), through the mounting plate (8), and a small air gap, returning to the solenoid through the split ring (4).

Fiber sleeves and washers insulate clamping bolts (A) from the electrode. Voltage is applied from a divider to mounting plate (8).

D. Filament Structure

The filament (10), a 0.035-in.-diam, 1/2-in. loop of tantalum, is mounted on two insulated copper rods (11). The ceramic seals (12) are soldered into the filament mounting plate (13). Alignment of this structure is insured by a recessed joint similar to that described above.

To change a filament, one removes bolts (B) and pulls the mounting plate off. The filament wire is set-screwed to the supports and a new one can readily be substituted.

Arc voltage is applied to the filament and, as mentioned above, the snout. Since the filament mounting plate is at snout potential, hydrogen, from a palladium leak, is fed to the source through an insulated joint on this plate.

E. Extractor Electrode

The extractor (14) is mounted on a spider (15). It can be replaced by removing the filament snout and aperture assemblies and inserting a collet extracting tool into the source body. The spider is rigidly mounted and, once aligned, will not move when the extractor is removed. Voltage is applied to the extractor through a vacuum feed-through. The extractor is Invar and the spider No. 316 stainless steel. A lens gap of 0.070 in. is normally used. This gap has held 100 kv for extended periods. Normal operating voltage is 70 kv. Figure 3 is an equipotential plot of the extracting field.

IV. SOURCE OPERATING CHARACTERISTICS

Figure 4 is a simplified circuit diagram of the source and electrode connections. The arc power supply is all solid-state and uses two triggered diodes. This supply is essentially a one-shot multivibrator and is triggered on and off. The output is 250 volts at 25 amp. Pulse length is variable, but is usually set at 1 ms. The repetition frequency is 2 pps.

The maximum field of the arc magnet is 3 kgauss. Normal operation is at about 1.2 kgauss. The magnetic flux in the snout aperture gap has not been measured, but may be quite high here.

Figure 5 is a plot of proton efficiency versus arc current. This is the percentage of ions. Neutral-atom efficiencies have not been measured. Normal arc operation is at 20 amp.

Figures 6 and 7 show arc volt-ampere curves and impedance for various magnetic field settings. Note that the arc impedance can be raised by increasing the magnetic field.

Figure 8 shows the effect of filament current on arc impedance. Normal volt-ampere shape is represented by the 68-amp curve. No adequate measurement of filament life has been made yet.

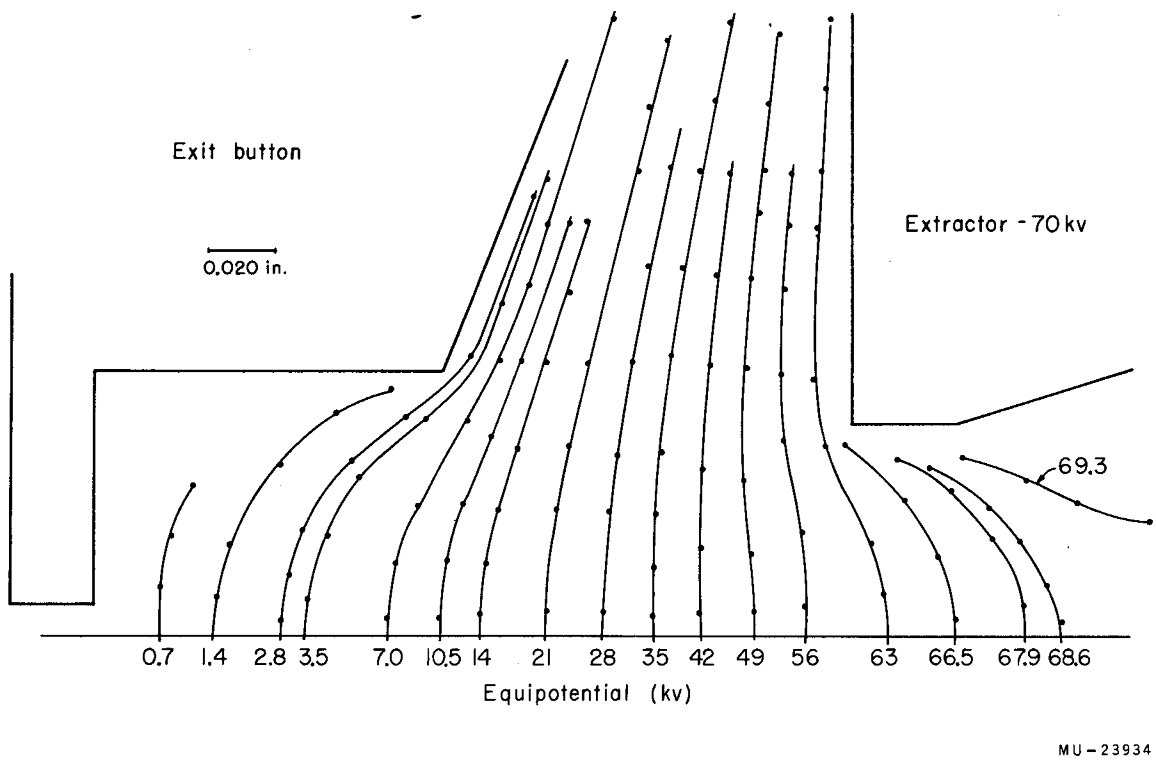

Fig. 3. Equipotential plot for the extraction electrode.

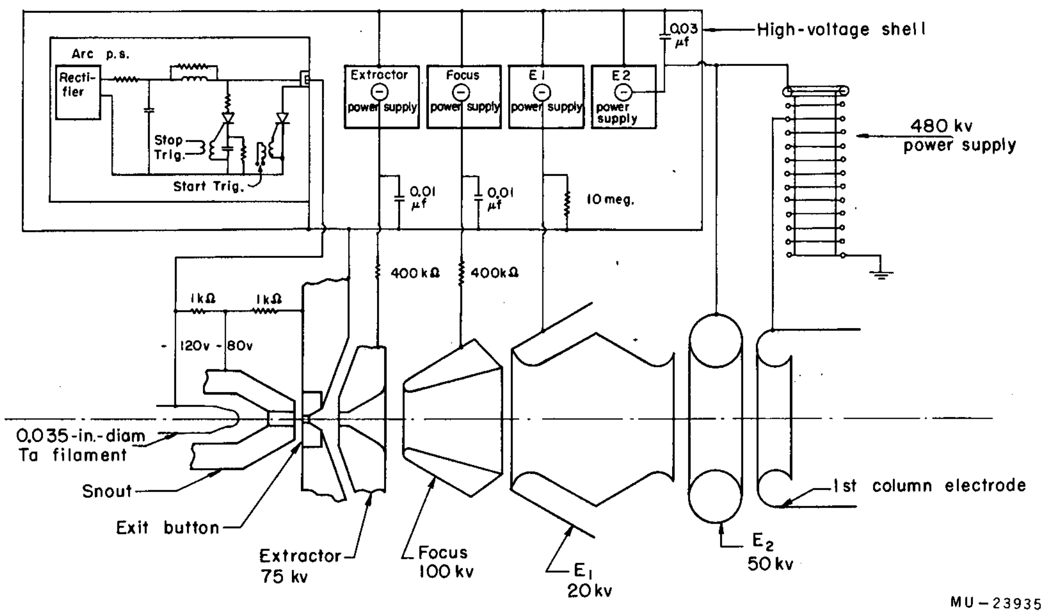

Fig. 4. Source and electrode connections.

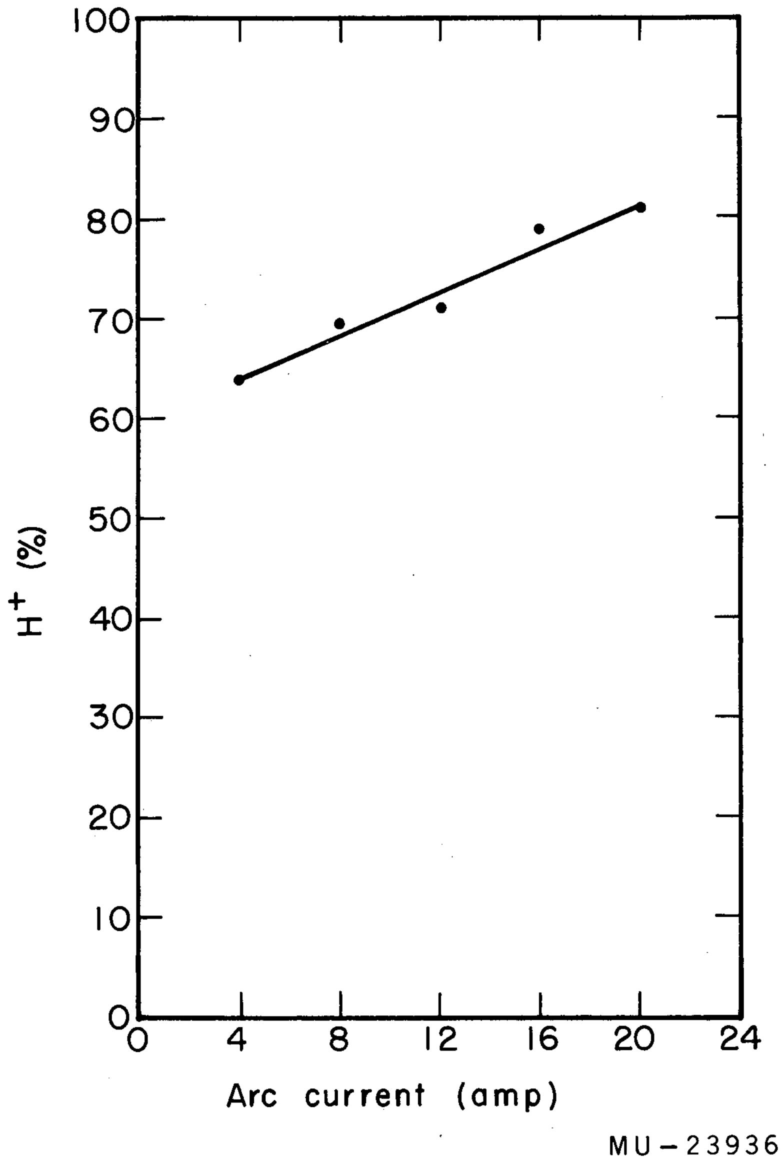

Fig. 5. Plot of H^+ efficiency versus arc current.

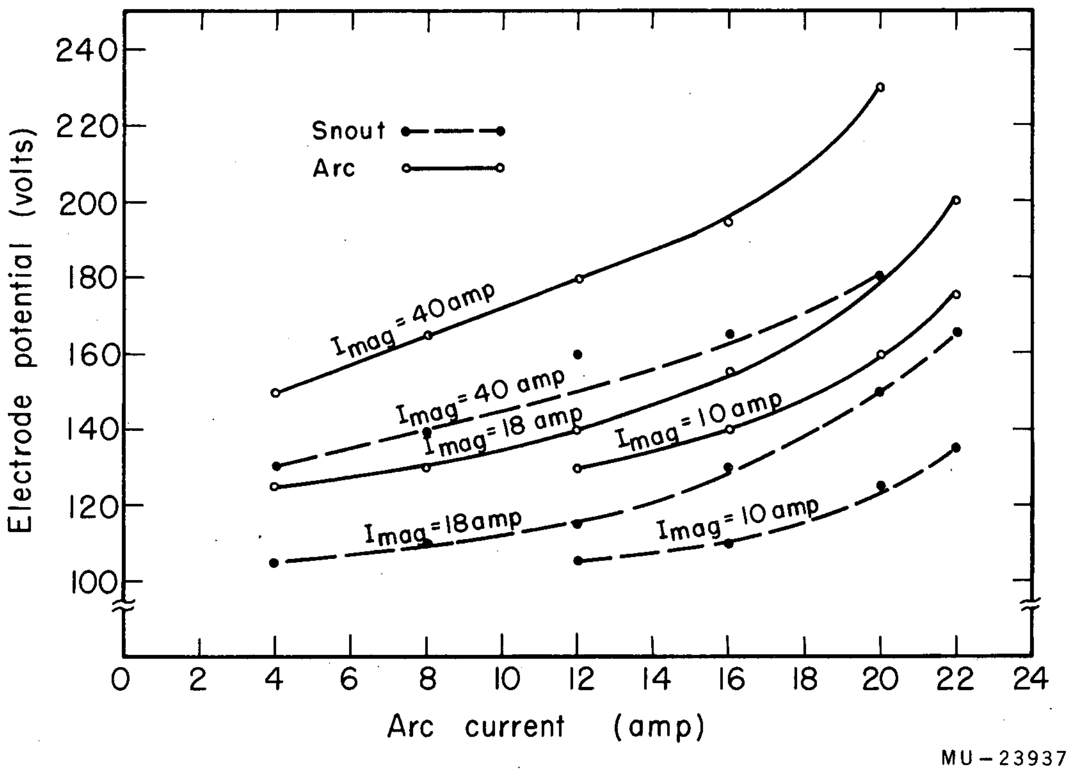

Fig. 6. Plot of arc and snout voltage versus arc current for a filament current of 63 amp.

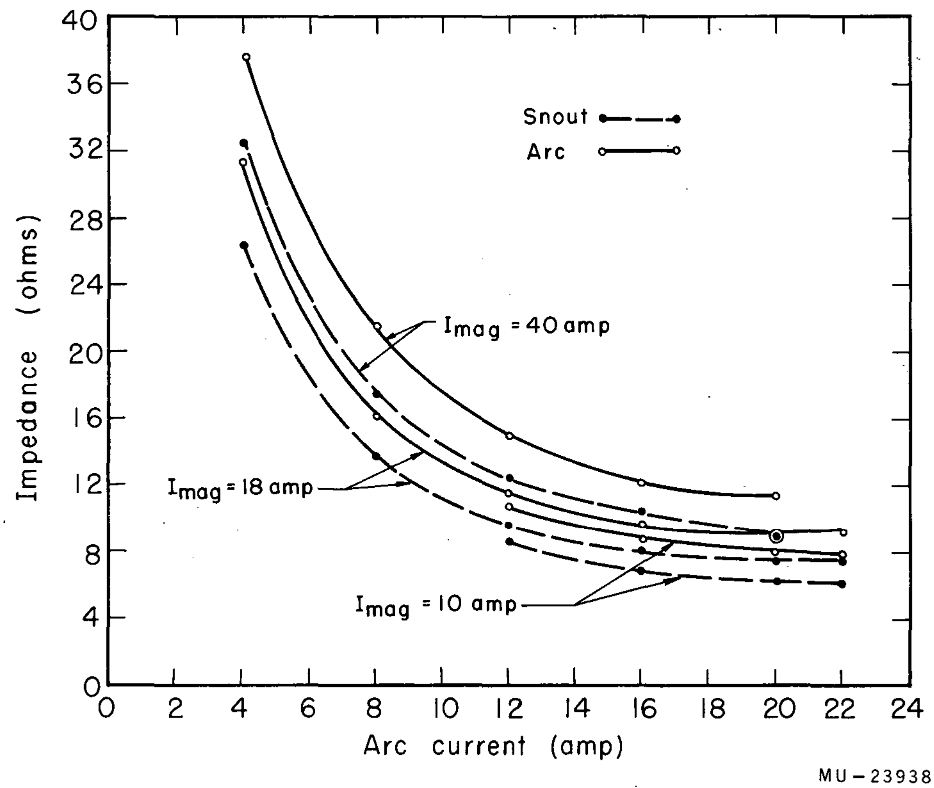

Fig. 7. Plot of arc and snout impedance versus arc current for a filament current of 63 amp.

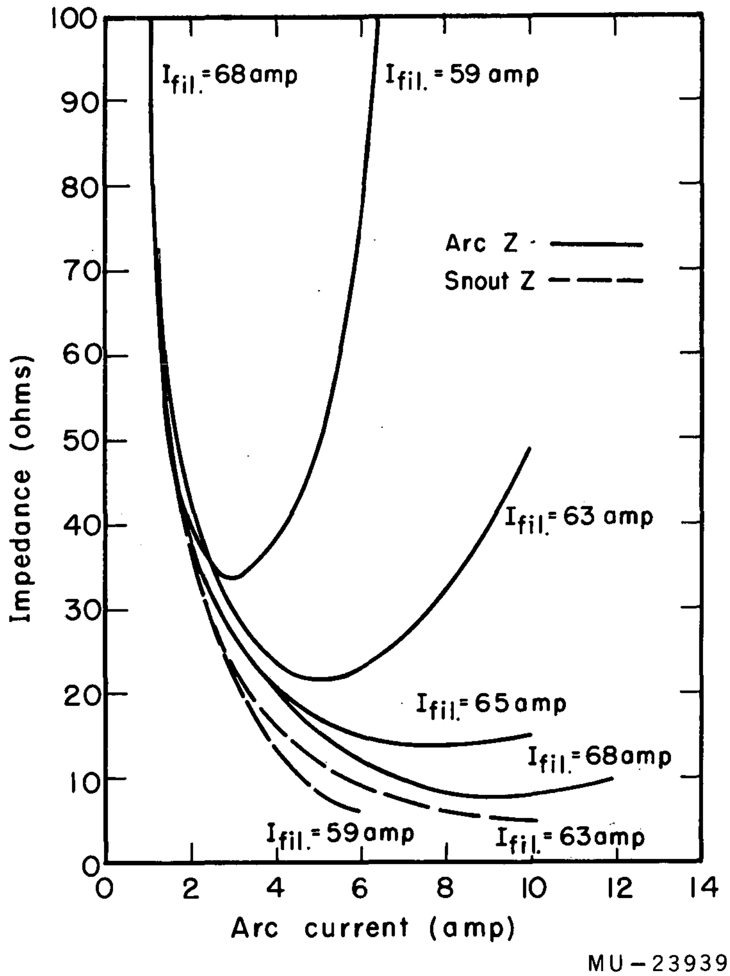

Fig. 8. Plot of arc and snout impedance versus arc current for various filament currents.

Maximum life appears greater than 48 hr.

Considerable work has been done on the extraction characteristics of the source. With the extraction geometry previously described, alignment of the snout with the aperture has a decisive effect. Table I summarizes the aperture characteristics with the snout, misaligned by 0.010 to 0.015 in. Table II shows the results obtained with proper alignment. An aligned snout permits use of a deeper aperture. This reduces the gas flow and allows operation at higher arc currents, increasing the proton efficiency.

The addition of a pump to the lens box increases the available beam by 20% (see Table II). We believe that raising the speed partially relieves a high-pressure region caused by gas emerging from the exit aperture.

In operation this source has been very stable, and 100 ma proton beams are readily attainable.

V. COCKCROFT-WALTON LENS DESIGN AND PERFORMANCE

A. Computational Methods

When it was decided to construct a high-intensity injector, it was apparent that the present electrostatic lens system would not handle the beam required.

The best way of obtaining beam orbits appeared to be the use of a wedge tank and a digital computer. Accordingly a tank was constructed and calibrated using the method developed by

Table I. Beam Extracted with Snout Misaligned

Aperture Diam.	Aperture Depth	Probe (kv)	Arc current (amps)	Beam (ma)
0.020	0.007	60	16	80
0.028	0.009	60	16	30

Table II. Beam Extracted with Snout Aligned

Aperture Diam.	Aperture Depth	Probe (kv)	Arc current (amps)	Beam (ma)
0.020	0.090	70	17	45
0.020	0.024	70	20	120
0.028	0.090	70	20	84

Table III. Effect of Pumping Speed on Beam[a]

Aperture (in.)	Pumping speed at probe ($l\ sec^{-1}$)	Beam at probe	Beam at column exit
0.028	30	40	30
0.028	100	50	42
0.040	30	Gas flow too high to run	
0.040	100	80	70

[a] Probe voltage: 50 kv.

Fechter and Striegl.[1] The tank was 24 by 20 in. and was accurate to 0.1% in the center and 1% near the walls, with a wedge angle of 2.5 deg. Electrode shapes were approximated by plane sections made of 1/16 in. copper.

Beam orbits were computed using an IBM 650 computer. In all cases a homogeneous beam of protons was assumed. The differential equation solved was

$$r'' + V'/2V\, r' + V''/4V\, r + \frac{20.58\, I}{V^{3/2}\, r} = 0 ,$$

where distances are in centimeters, V in kilovolts, and I in amperes. Primes indicate derivatives with respect to Z.

In practice, the electrode system was modeled in the tank, and the potential variation along the axis was obtained. This was fed into the computer, and the necessary derivatives were calculated, using finite-difference expressions. In addition, the beam radius and divergence at the second field point was assumed. From the orbits obtained and an equipotential plot we were able to get the desired lens shapes.

B. Column Design

Two types of accelerating columns were investigated. These were the standard linear-gradient column and the power-law column of Harrison.[2] Theoretically the Harrison column will confine an intense beam; however, it would be difficult to construct one for 500 kev. Therefore we decided to use the linear accelerating tube and to design a lens that would match the source and column.

The beam characteristics were studied by ray tracing backwards through the column. The final energy was 480 kev and the entrance energy was set at 60 kev. This was determined by the expected voltage stand-off characteristics of the new injector. Figure 9 shows some typical orbits.

Results of the calculations are shown in Table IV for 30- and 10-cm columns. In order to obtain these input conditions, it was necessary to correct for the converging effect of an ion entering a field region.[3] Input conditions for the two cases are similar. A large (approx 6-cm diam) convergent beam is required. The column being used is 76-cm long, 7.62 cm in diameter, with a gradient of 538 kv M^{-1}.

C. Matching Lens Design

Figure 10 is a drawing of the lens used to match the source and column. It is a four-electrode accel.-accel.-decel.-accel. type. The beam emerging from the source is accelerated to about 100 kev by the extractor and focus electrodes. Then the beam is decelerated by the E_1-focus gap to increase its radius. This gap is converging so that a balance can be obtained between the lens focusing forces and the beam blow-up, thereby allowing control of the radius. The E_1-E_2 gap and the first column gap give the beam a radially inward push, causing it to become slightly convergent, while accelerating it to the proper column-injection energy.

Figures 11 and 12 show the lens equipotentials as well as the axial potential and its first and second derivatives. The

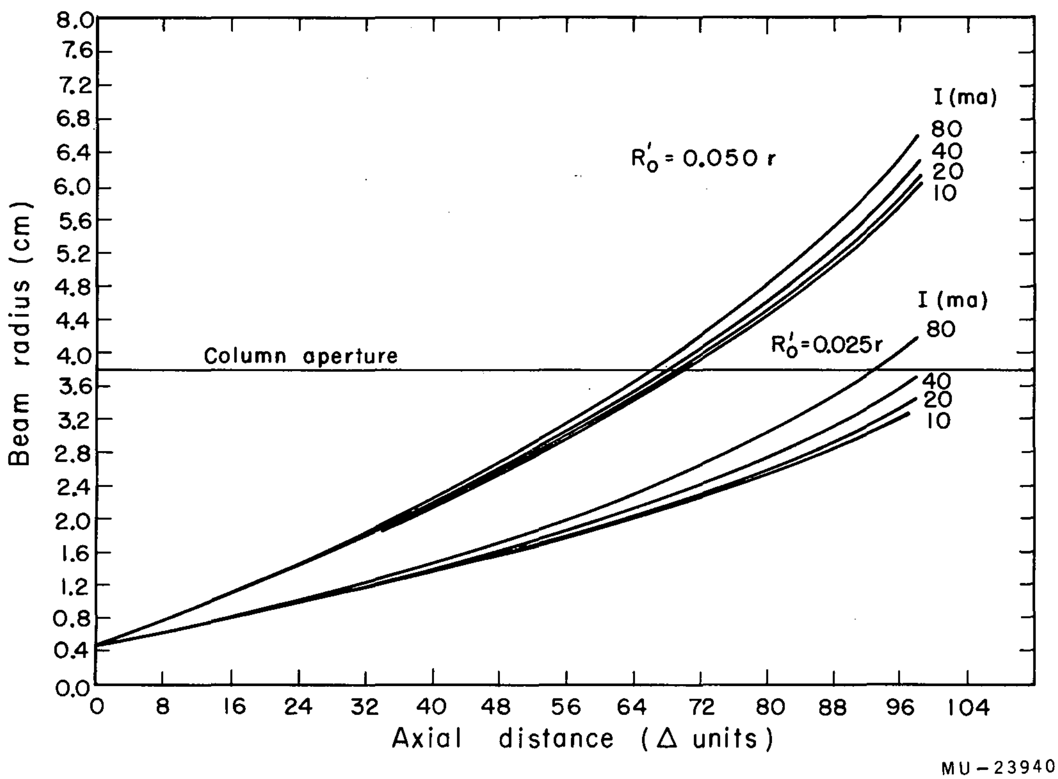

Fig. 9. Column backtrace—beam envelopes as a function of output convergence R_o', where R_o is 0.5 cm and Δ is 0.762 cm.

Table IV. Input conditions for comparison of high and low gradient columns

Low gradient (538 kv/m)					High gradient (4100 kv/m)		
I (ma)	R (mm)	θ[a] (mrad)	Initial Beam conditions[a] R'(mrad)	R(mm)	I (ma)	R (mm)	θ[a] (mrad)
5			– 10	10	5	18.9	–13.9
10	20.7	12.3			10	19.1	–14.5
20	21.9	8.99			20	19.6	–15.8
30					30	20.1	–17.1
40	24.1	2.65			60	21.4	–20.3
80	28.3	–8.19			80	22.3	–22.7
100					100	23.3	–26.5
200					200	27.5	–34.9
5			– 0	10	5	13.5	– 9
10	14.6	10.			10	16.1	–16
20	15.9	7.2			20	20.9	–27.7
30					30	25.4	–33.5
40	18.4	2.2			40	29.6	–47.2
80	23.1	–10.4			80	44.2	–77.8
100					100	50.8	–91.7
5	0.89	5.5	10	10	5	3.2	8.6
10	2.1				10	3.6	7.3
20	4.2	.93			20	4.4	4.9
30	6.0	– 4.6			30	5.1	2.7
60	10.9	–17.3			60	7.2	– 3.0
80	13.6	–22.8			80	8.4	– 6.5
100	16.3	–28.5			100	9.6	–17.6
200	27.3	–48.9			200	15.2	–23

[a] Minus sign is convergent beam.

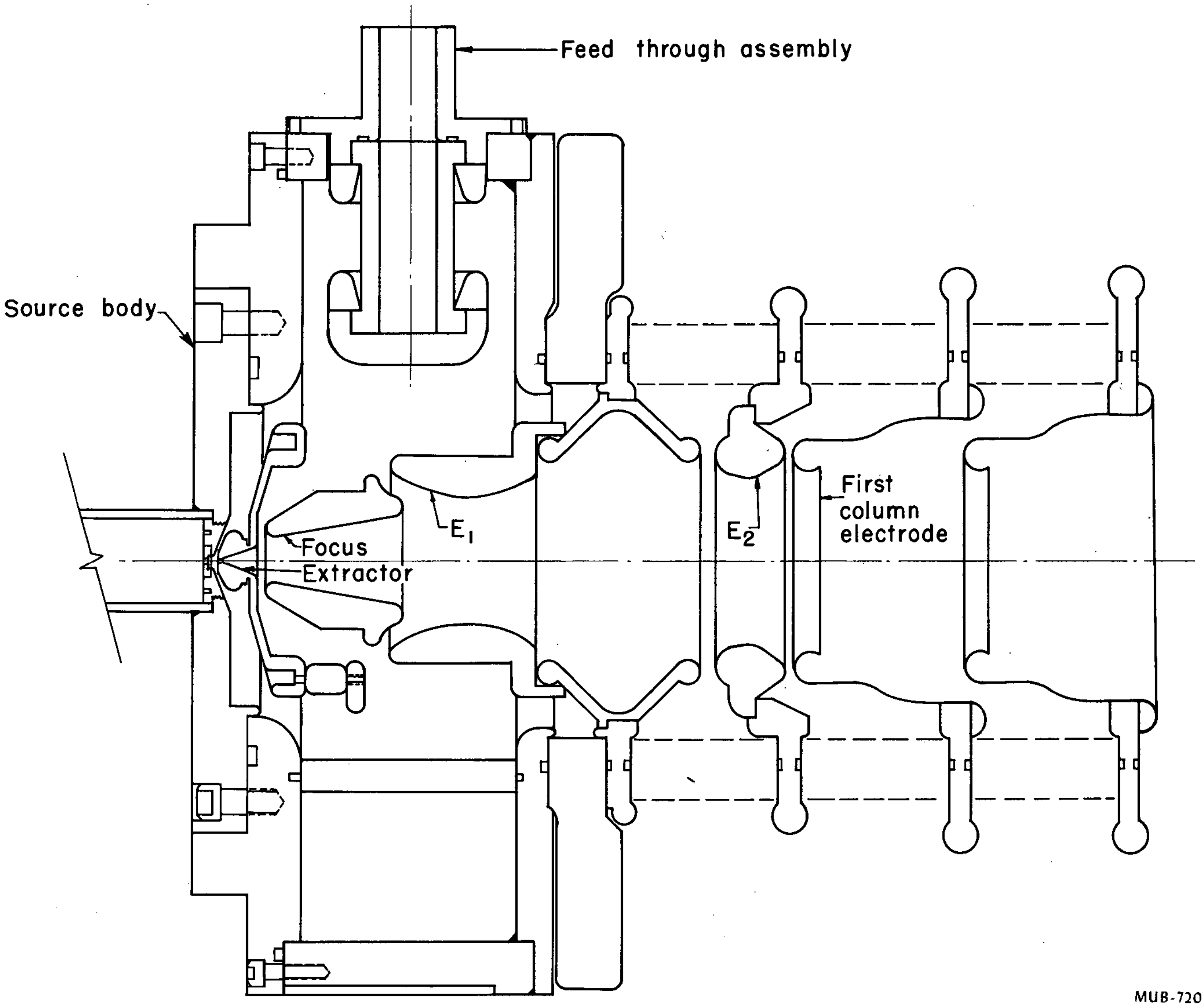

MUB-720

Fig. 10. Four—electrode lens assembly.

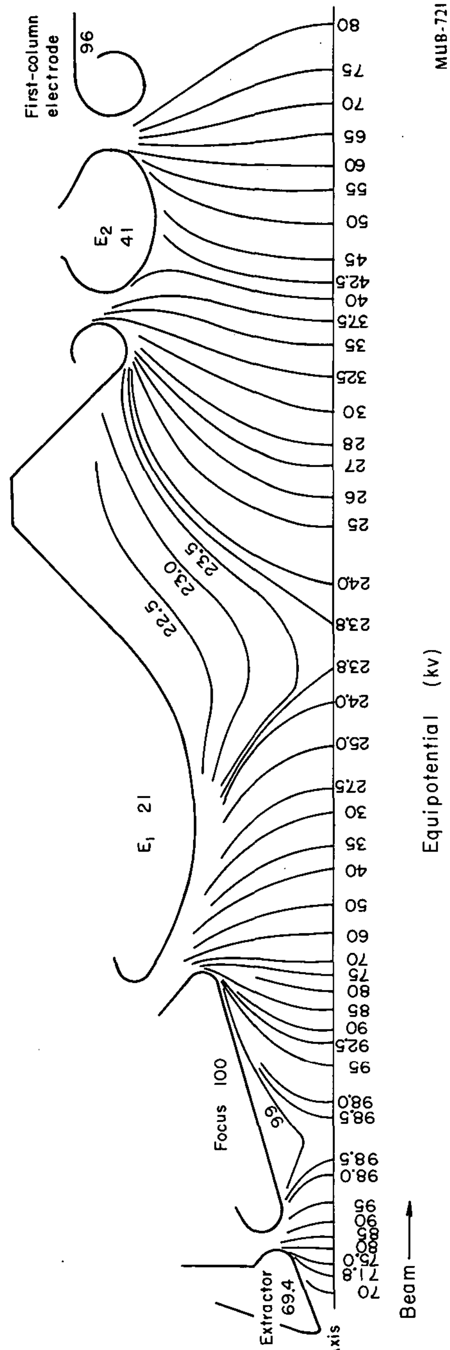

Fig. 11. Equipotential plot for injector four-electrode lens.

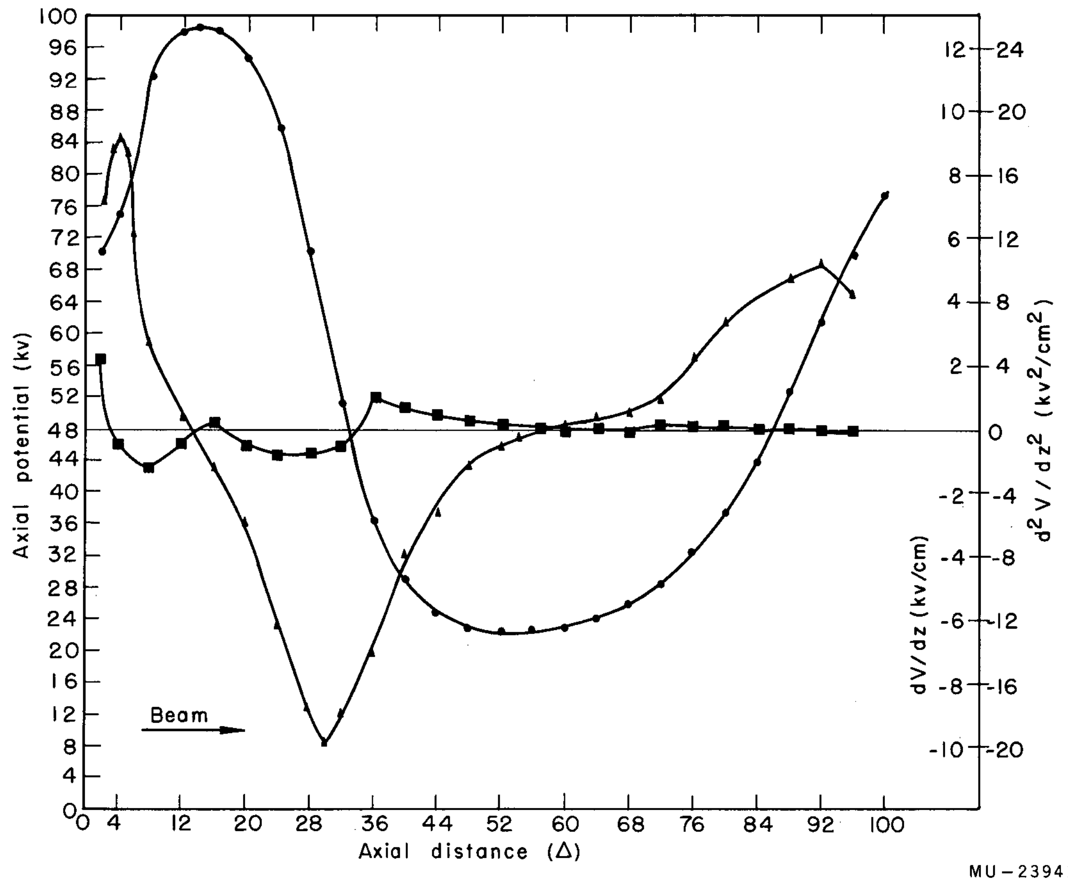

Fig. 12. Potential plots for injector four—electrode lens. Extractor potential is 70 kv; focus potential, 100 kv; E_1 = 21 kv; and E_2 = 55 kv. Symbols denoting $\bar{V}$, dV/dz, and $d^2\bar{V}/dV^2$ are 0, △, and respectively.

large curvature of the off-axis equipotentials helps to keep the beam well-confined.

Typical beam orbits are shown in Figure 13. The currents all have the same initial conditions ($R_o = 0.25$ cm and $R_o' = 7$ deg). At the voltages used there is no crossover.

Figure 14 shows profiles through a 175-ma beam. The initial radii are separated by 0.05 cm and the divergences used are the angles subtended by the radii and the distance of the probe from the source aperture. There appears to be no major distortion in the orbits.

D. Lens-System Performance

This lens has performed well. We have achieved a total beam of 150 ma at 1 in. from the column exit. The waist diameter was 1.6 cm, and 80% of the beam was within a diameter of 1 cm. The beam profiles show some loss on E_2; this has been observed experimentally. However, 90% of the beam is transmitted through the lens.

E. Lens-Assembly Details

The column electrodes, including E_1, E_2, and the lens tank, are stacked on an alignment mandrel. Six metal rods compress the entire assembly prior to its placement on the test stand.

The high-voltage end of the unit is supported by an adjustable bipod, and the ground end is fitted to solenoid M 1 with a precision joint. Two thrust bolts allow column compression to be maintained while the six rods are removed.

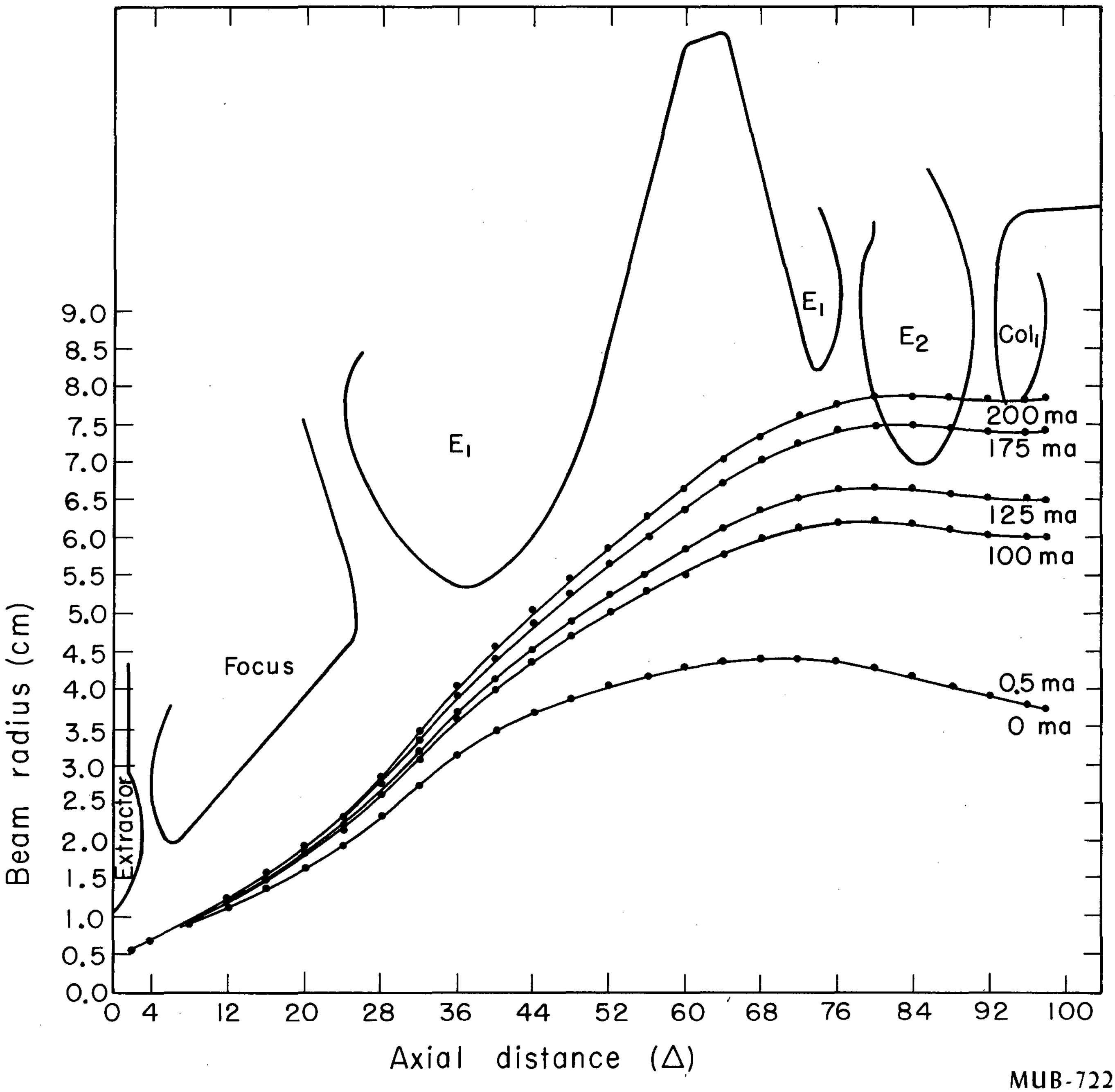

Fig. 13. Beam envelopes for injector four-electrode lens. Extractor potential is 70 kv; focus potential, 100 kv; E_1 = 21 kv; and E_2 = 55 kv.

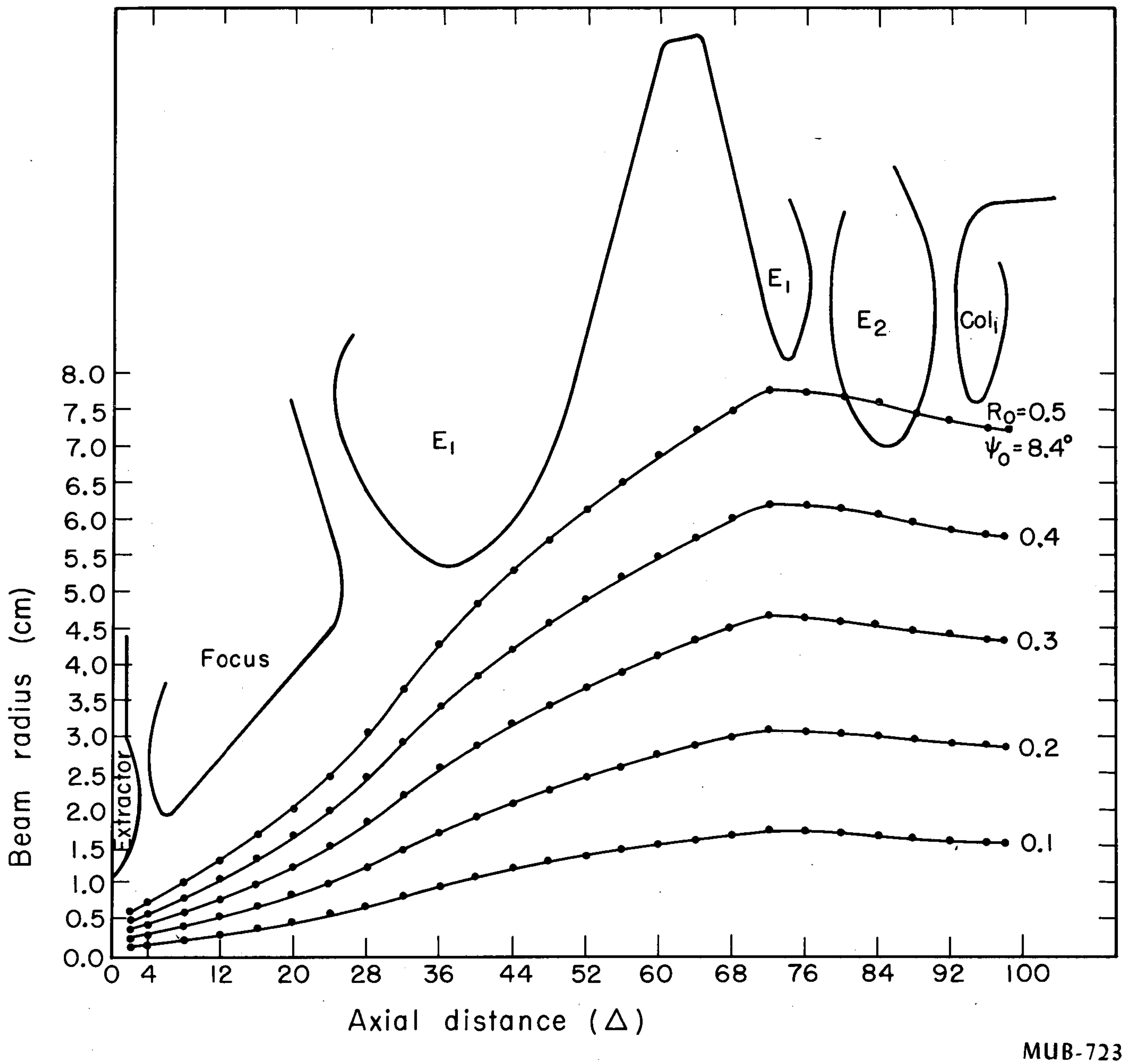

Fig. 14. Beam profile for a homogeneous 175–ma beam with injector four–electrode lens. Extractor potential is 70 kv; focus potential, 100 kv; E_1 = 21 kv; E_2 = 55 kv; and the first–column voltage is 112 kv.

A precision optical level is used to establish the column axis on a level line of sight. Adjustments are provided on the lens tank feed-through to allow the extractor and focus electrodes to be positioned accurately. The source then bolts onto the rear of the lens tank and is aligned by a precision joint. With this technique, electrode concentricity within ± 0.002 is assured.

VI. BEAM-TRANSPORT SYSTEM

Because space-charge effects are still large at 500 kev, it was necessary to construct a beam-confining system. We used solenoidal focusing because of its simplicity. This, of course, has the disadvantage of requiring high-power magnets.

Figure 15 is a layout of the transport system. Two solenoids are used. The first one is an integral part of the column assembly. It is located as close to the column waist as possible. This magnet is 10-3/4 in. long and has an inside diameter of 3 in. It is wound in eight layers with 23 turns per layer. The coil leads are brought out to permit maximum cooling. In winding, considerable care must be used to insure coil uniformity. Otherwise the lens will have large aberrations. Figure 16 is a typical field profile. This magnet has a coil resistance (parallel connection) of 29 milliohms (mΩ) and a peak field of 9.8 kgauss at 1 ka.

The second magnet is placed 33 in. from the exit of the column solenoid. This magnet is 20 in. long and has a 2-in. inside diameter. It has a coil resistance of 21 mΩ. The peak

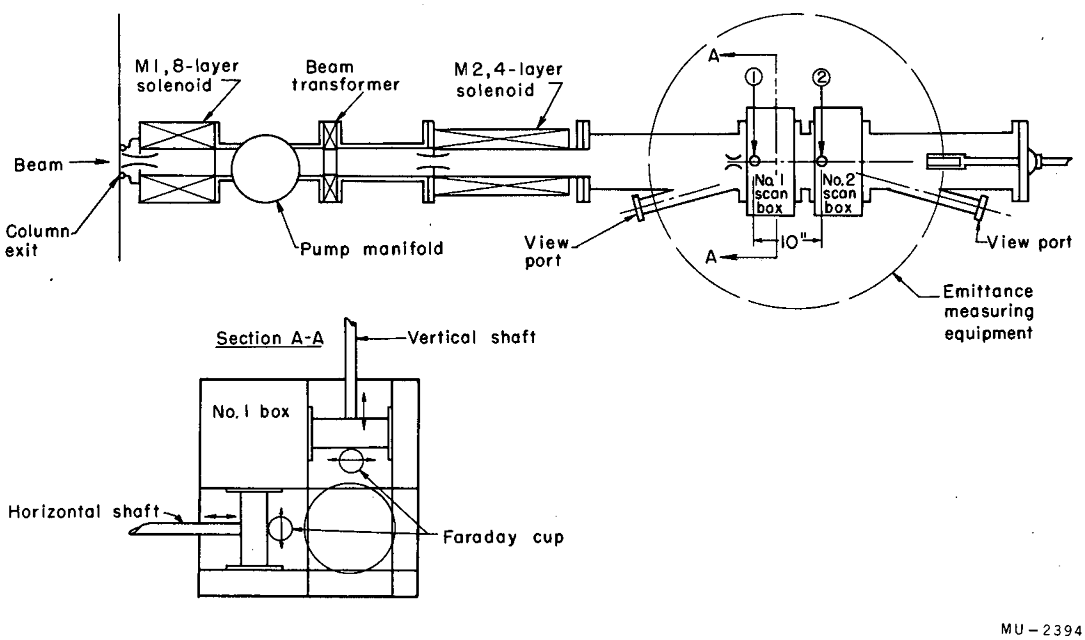

Fig. 15. Typical beam transport system.

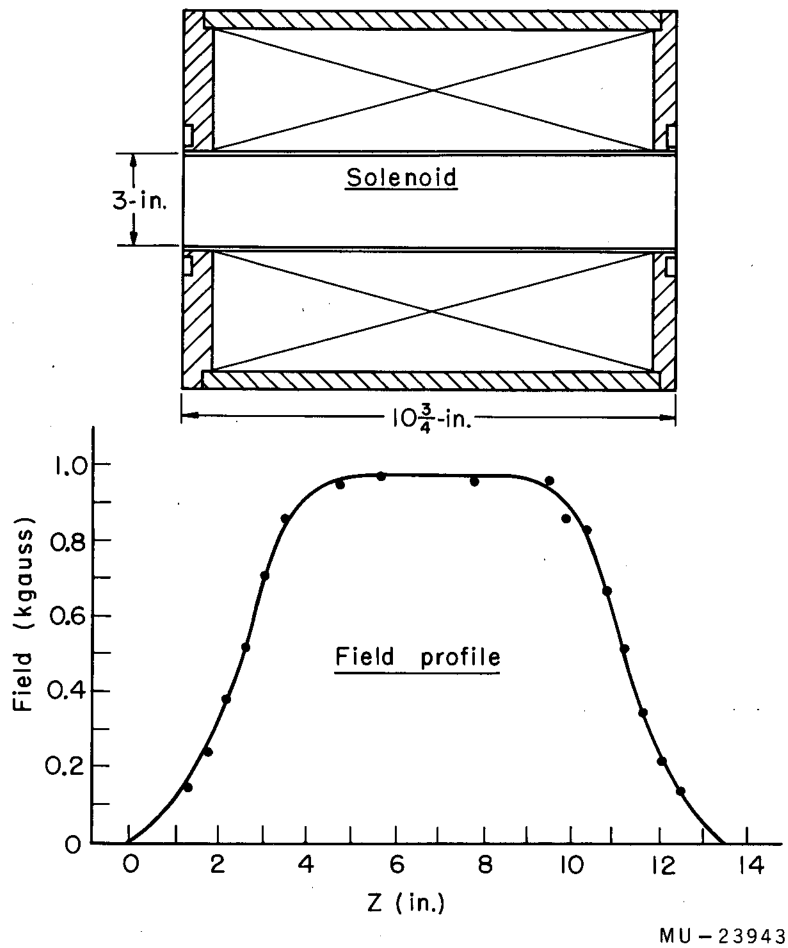

Fig. 16. Section of solenoid M 1 and field profile for a 102—amp solenoid current.

field is 7 kgauss at 1 ka.

With these magnets we have achieved 85 ma of protons 82 in. (point 1, Figure 15) from the exit of the first solenoid.

VII. BEAM-QUALITY MEASUREMENTS

At the foci of the two solenoids we have determined the emittance of the beam and its proton content.

The emittance measurement was made in a manner analogous to that of Marsicanin and Tallgren.[4] Figure 15 shows a typical set-up. We determined the center of gravity of the beam by scanning at points (1) and (2) with two Faraday cups. The beam was focused slightly ahead of point (1). The cup apertures were 1 mm diam. A 1-mm aperture was inserted at point (1) and moved along the X and Y axes of the beam. At each aperture position, the beam zeros were measured by the cup at point (2). Then the divergence of the beam was calculated by transforming the aperture location from point (1) to point (2) and dividing by the cup separation.

Figures 17 through 20 show the X and Y emittances for both magnet foci.

Hereward at CERN has calculated that the acceptance of their linear accelerator is 179 mrad-mm, and our beam appears to be within these limits. Ninety percent of the beam is within a diameter of 4.3 mm and has an emittance of 73 mrad-mm.

The beam amplitudes of the two foci are those obtained when the complete transport system is operated; that is, there is

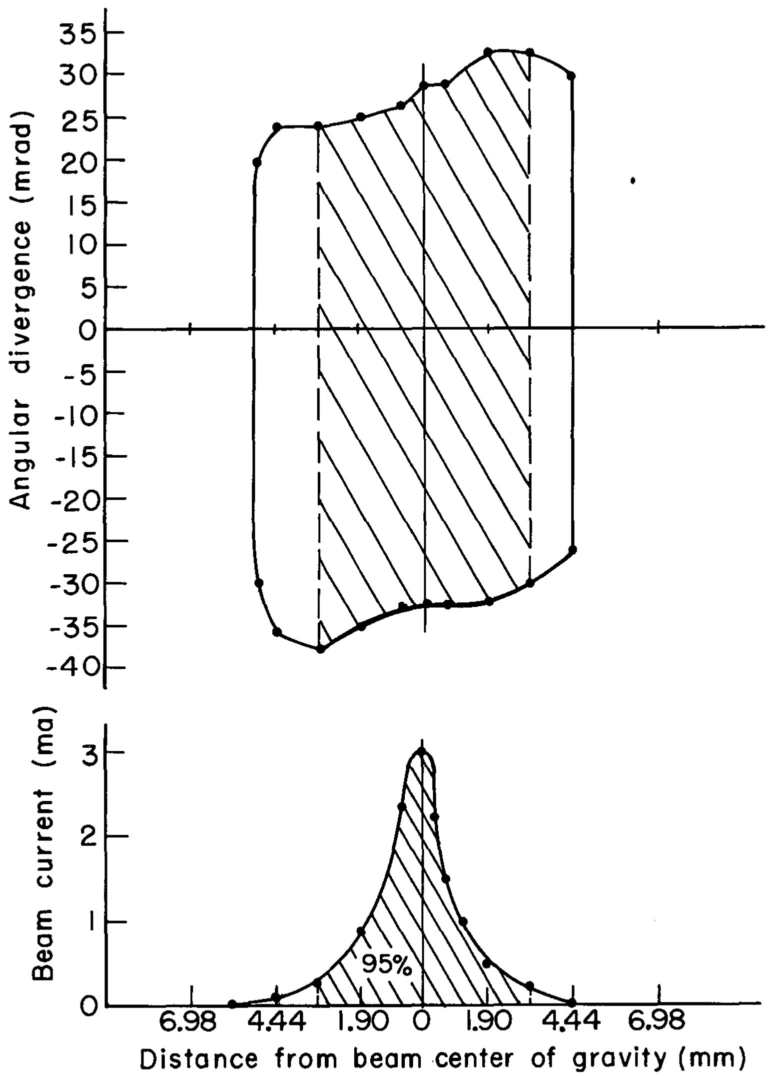

MU-23944

Fig. 17. X emittance at first focus for 95-ma proton beam.

	370 kev	500 kev
Emittance of total beam	178 mrad-mm	154 mrad-mm
Emittance of 95% of total beam	128 mrad-mm	109 mrad-mm

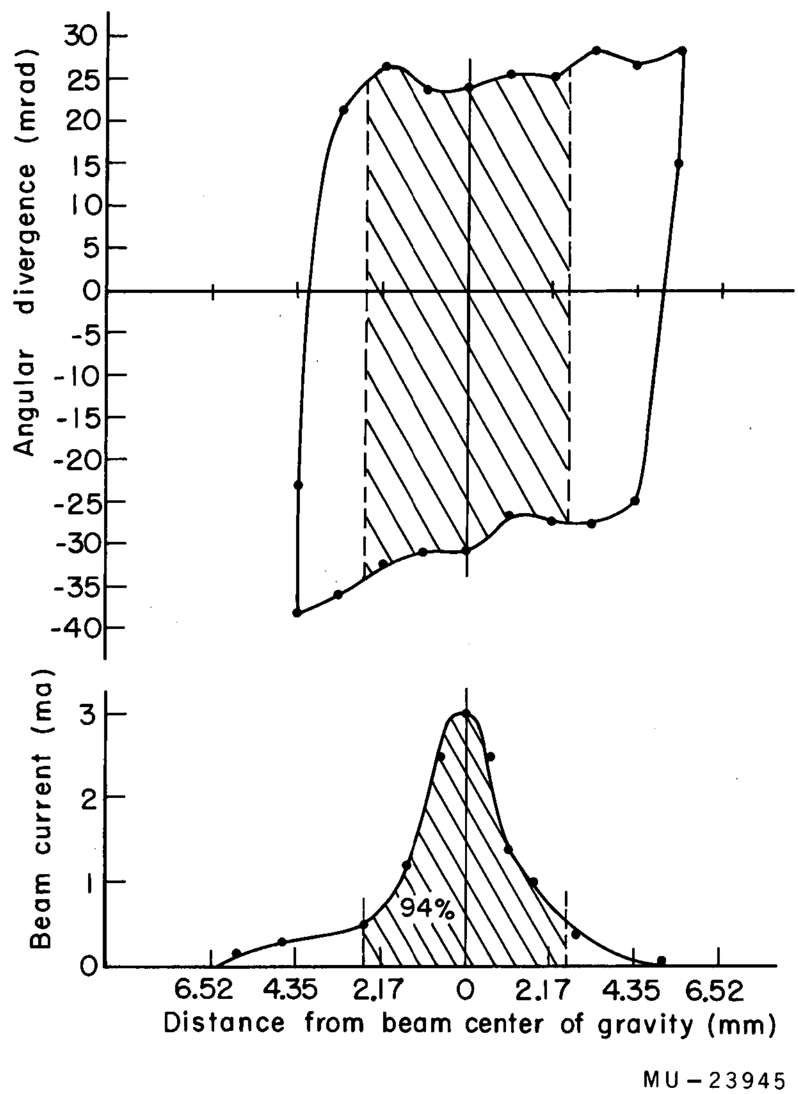

Fig. 18. Y emittance at first focus for 95-ma proton beam.

	370 kev	500 kev
Emittance of total beam	156 mrad-mm	136 mrad-mm
Emittance of 94% of total beam	83.5 mrad-mm	73 mrad-mm

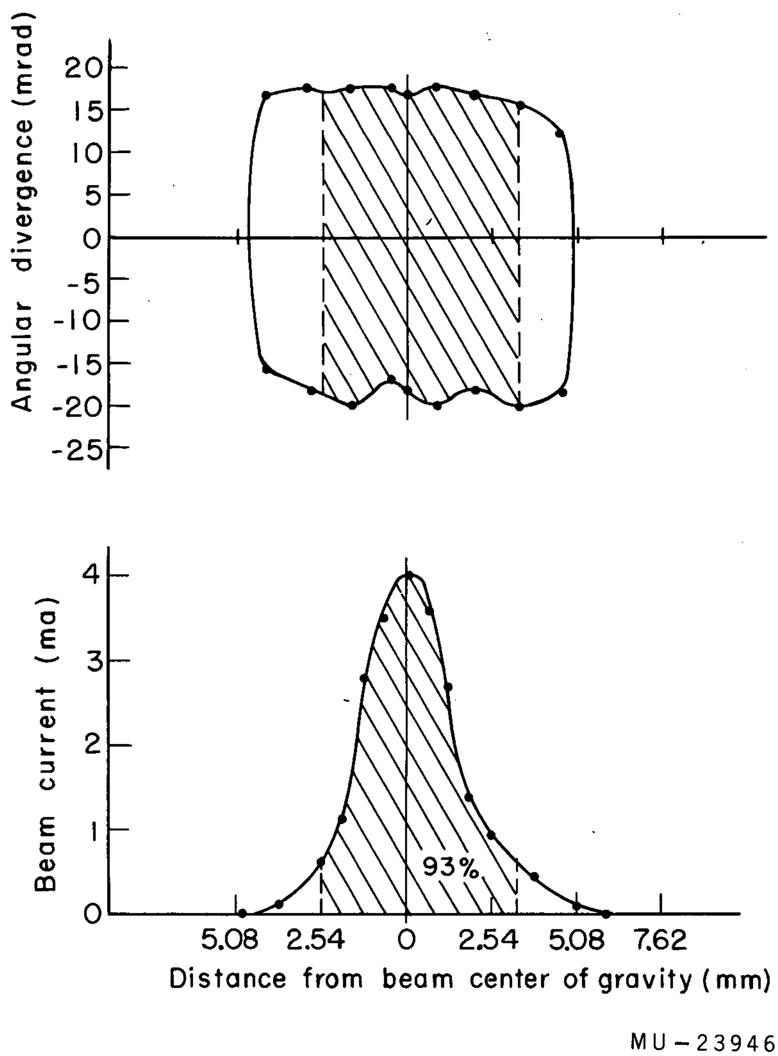

Fig. 19. X emittance of second focus for 80-ma proton beam.

	375 kev	500 kev
Emittance of total beam	105 mrad-mm	91 mrad-mm
Emittance of 93% of total beam	67 mrad-mm	58 mrad-mm

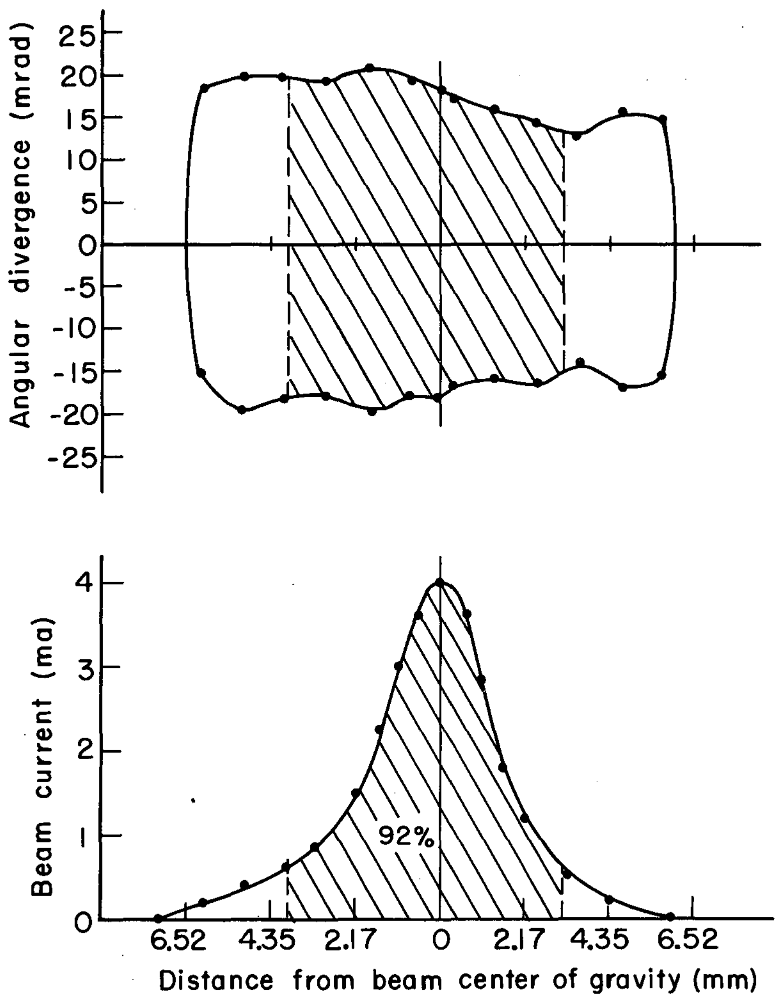

Fig. 20. Y emittance at second focus for 80-ma proton beam.

	375 kev	500 kev
Emittance of total beam	127 mrad-mm	110 mrad-mm
Emittance of 92% of total beam	73 mrad-mm	63 mrad-mm

a 10% beam loss through the second magnet. All measurements were made at the stable voltage limit of the test stand. This was at 370 kev. The maximum voltage run with beam was 410 kev. This limit is due to room geometry and not to the column structure, e.g., sparkdown was from the shell to the room floor.

A mass spectrograph has been set up and the beam purity determined at the foci. Figures 21, 22, and 23 show the results. The instrument had a resolution of ± 1 amu at mass 30. Identification of the proton peak was done by wire orbiting. The deflection angle was 20 deg. It is of interest to note that the magnets apparently analyze the beam. We have obtained results like these, with a source efficiency of 60%. The first small peak is probably low-energy protons, created by the dissociation of H_2^+ in the column.

We have obtained 120 ma of protons at the first focus, with an arc current of 20 amp.

Beam intensity has been measured using a shielded Faraday cup and a beam transformer. The cup and transformer agree, so long as the cup is 4 in. or more downstream from the transformer. Otherwise secondaries from the cup face cause the transformer to read high. We have not been able to get a good bias plateau, but as Figure 24 shows, there is a slight plateau at -10 v bias.

A calorimeter is being constructed, and will be used to further check our intensity. With 80 ma incident on the cup at 370 kev, the cup was an orange-red color. This is with a duty cycle of 2×10^{-3}.

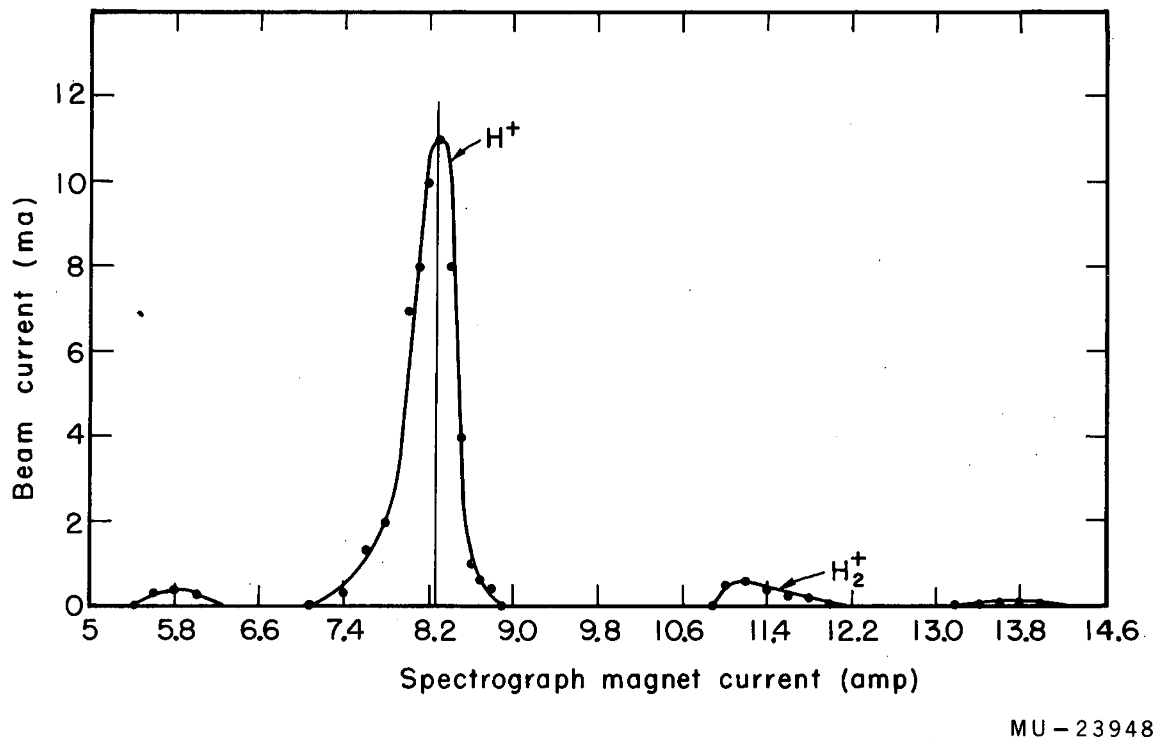

Fig. 21. Plot of beam current versus spectrograph magnet current at first focus. The M 1 solenoid current, 394 amp, is adjusted for maximum H^+ beam into a 3/4-in.-diam cup. Beam energy is 345 kev.

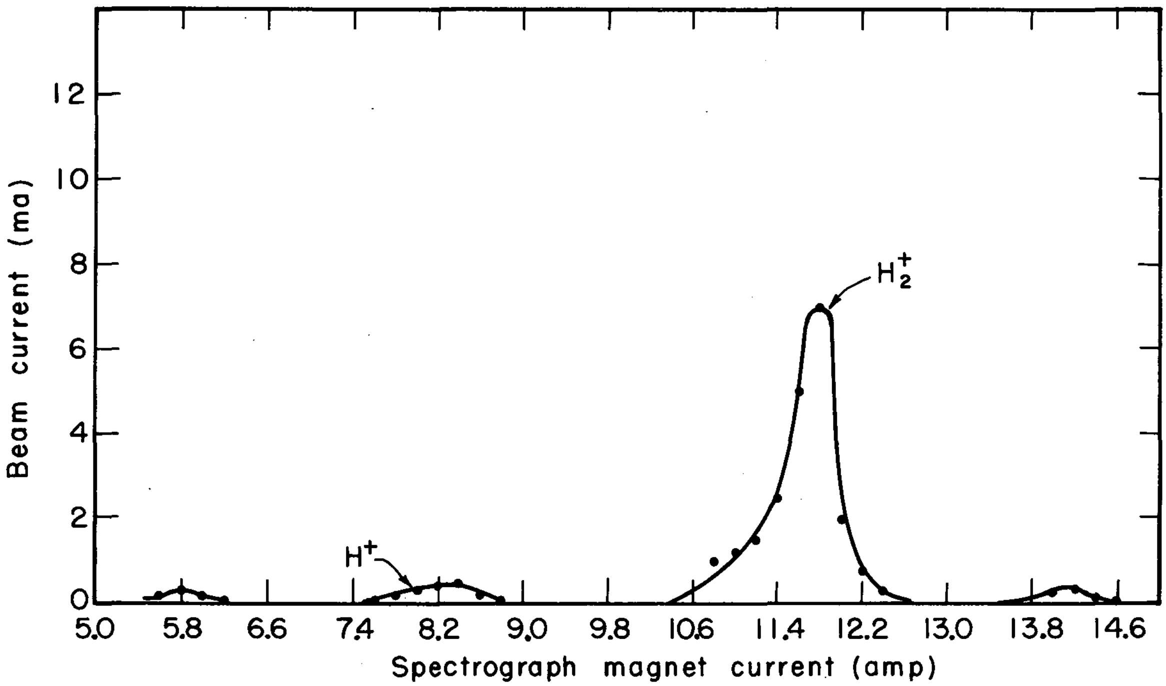

MU-23949

Fig. 22. Plot of beam current versus spectrograph magnet current at first focus. The M 1 solenoid current is adjusted for maximum H_2^+ beam into 3/4-in.-diam cups. Beam energy is 345 kev. The M 1 solenoid current is 568 amp.

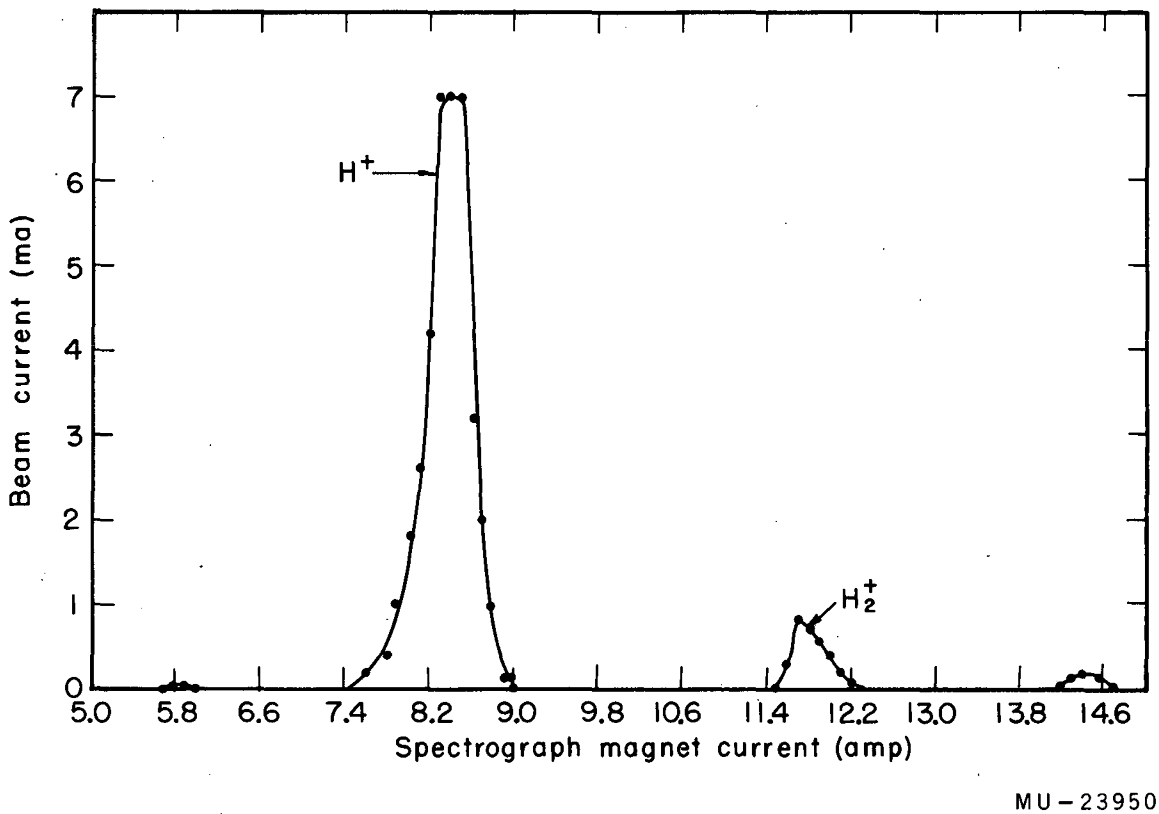

Fig. 23. Plot of beam current versus spectrograph magnet current at the second focus. Solenoids M 1 and M 2 are adjusted for maximum H^+ beam into 3/4-in.-diam cup. Beam energy is 370 kev. The M 1 solenoid current is 376 amp. The M 2 solenoid current is 570 amp.

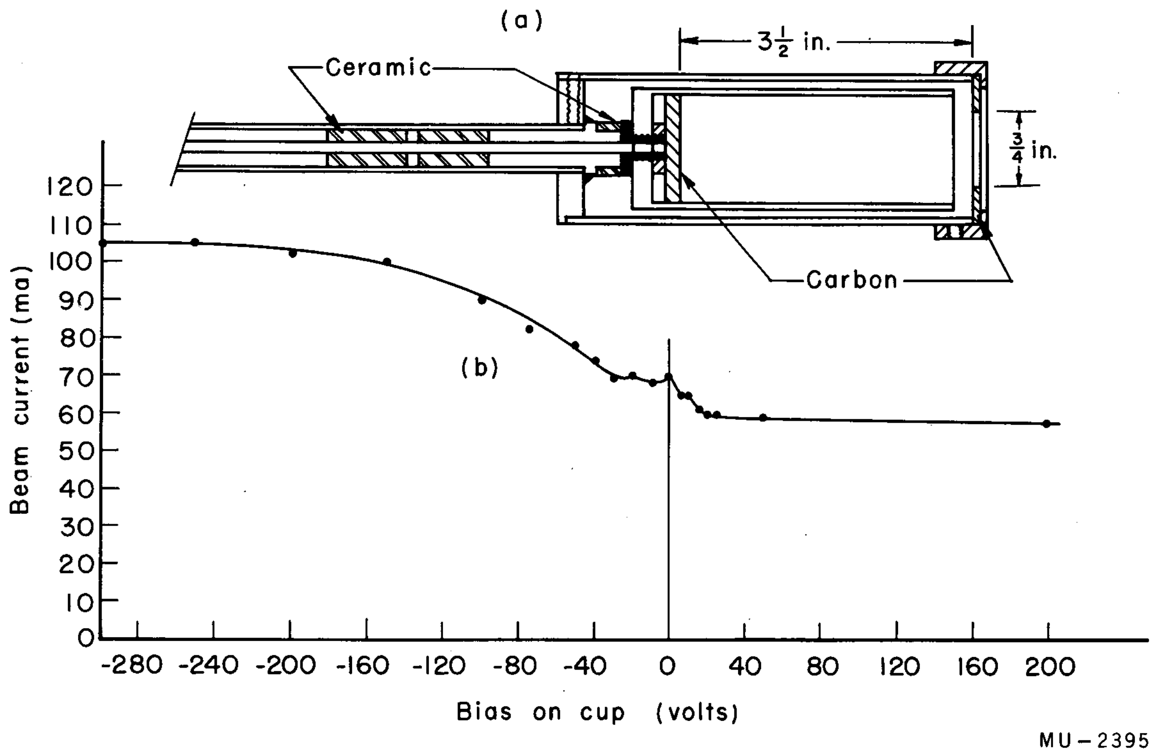

Fig. 24. (a) Cross section of Faraday cup.
(b) Plot of beam current versus bias volts on cup. Beam current is 70 ma.

ACKNOWLEDGMENTS

Many people participated in this project. We especially would like to thank Dr. Hugh Hereward for freely giving us his experiences with the CERN injector, and Dr. Malcolm McGregor for checking our field-plotting methods with his iteration program. Messrs. Robert Force and John Barale, from the Bevatron Engineering Group, gave us invaluable assistance with our electronics. Many of the Bevatron Crew members have helped us in assembly and data reduction.

REFERENCES

1. H. R. Fechter and M. Striegl, Electrolytic Tank Construction, Calibration, and Applications, Particle Acceleration Division, Argonne National Laboratory, HF-MS-1, October 13, 1958.
2. E. R. Harrison, Some Notes on the Acceleration of Relatively Large Current Proton Beams, AERE G/R 991, September 9, 1952.
3. C. J. Davisson and C. J. Calbick, Phys. Rev. 38, 585 (1931), Chaps. I, IV, and X.
4. B. Marsicanin and V. Tallgren, Preliminary Emittance Measurements on the Pre-Injector, P. S. Int. Lin. 59-24, CERN, August 24, 1959 (unpublished report).